Original Research

Grain Size Engineering and Enhanced NO_x Sensitivity in RF-Sputtered Indium-Doped Zno Thin Films

M. Vanmathi [1], A. Priya [1], P. Ponnusamy [2], M. Senthil Kumar [2,*], V. Elango [3], T. Athisaya Anushya[1]

[1] Department of Electronics and Communication, B S Abdur Rahman Crescent Institute of Science and Technology, Chennai, Tamil Nadu, India – 600 048;
[2] School of Mechanical Engineering, VIT University, Chennai, Tamil Nadu, India – 600 127;
[3] Department of Robotics and Automation, Easwari Engineering College, Chennai, Tamil Nadu, India – 600089.
* Correspondence: msv305@yahoo.co.in

Received: December 29, 2025; Accepted: May 11, 2026

Abstract: Indium-doped zinc oxide (In:ZnO) thin films are promising materials for NO_x gas sensing due to their tailorable electrical properties and enhanced surface activity. In this study, ZnO thin films doped with 1–8 at% indium was deposited on glass substrates using radio-frequency magnetron sputtering to investigate the influence of dopant incorporation on structural, electrical, and NOx gas-sensing characteristics. X-ray diffraction analysis confirmed the formation of a hexagonal wurtzite ZnO structure with a preferred (002) orientation. Indium doping induced peak shifting and broadening, indicating lattice distortion caused by the substitution of In^{3+} ions without secondary phase formation. Grain size estimation using the Scherrer equation revealed an average crystallite size of ~25 nm for pure ZnO, which decreased to ~20 nm upon indium incorporation due to suppressed grain growth. Scanning Electron Microscopy (SEM) analysis revealed the surface morphology and microstructural evolution of In:ZnO thin films, indicating uniform grain distribution and enhanced crystallinity with doping concentration. Electrical resistivity strongly depended on indium percentage, with moderate doping enhancing carrier concentration, while higher doping levels led to mobility degradation due to increased scattering. Static NO_x gas sensing measurements demonstrated significantly enhanced sensitivity for films doped with 2–6 at% indium at reduced operating temperatures, attributed to increased oxygen vacancy concentration, improved surface reactivity, and optimized microstructure. These results identify an optimal doping window and establish RF-sputtered In:ZnO thin films as efficient candidates for advanced NO_x gas sensor applications.

Keywords: thin films; electrical conductivity; resistivity; gas sensing.

1. Introduction

Indium-doped zinc oxide (In:ZnO) thin films have attracted great interest recently for their tunable electrical, microstructural and gas-sensing characteristics, especially for nitrogen oxides (NO_x) detection, which are environmentally critical pollutants associated with vehicular emissions, industrial combustion and atmospheric photochemical processes [1–3]. ZnO, with a wide band gap of 3.37 eV, belongs to the II–VI semiconductor family and has been widely adopted in optoelectronic and sensing applications due to its rich defect chemistry, strong surface charge modulation capability and excellent chemical stability [4,6]. However, ZnO typically suffers from baseline conductivity, insufficient active defect states and relatively slow response–recovery dynamics when exposed to strongly oxidizing gases such as NO_2 [5,15]. Therefore, doping strategies have become one of the most effective approaches to tailor the electrical conductivity, grain boundaries, surface chemisorption behaviour and defect states of ZnO to enhance its gas sensing performance [1,7–9].

ZnO defects, carrier concentrations, and adsorption sites gets significantly impacted by doping it with aliovalent cations (Al^{3+}, Ga^{3+}, In^{3+}, Sn^{4+}, and other transition metal ions). This can increase sensitivity of the operating temperature. Group III elements (Al, Ga, and In) used as doping agents work as donors to boost free electron concentrations as well as oxygen vacancy levels in ZnO, which serve as gas adsorption sites [10]. This boost to charge transfer between gas molecules is very essential in the detection of oxidative gases, particularly NO_x.

Among various dopants, indium (In^{3+}) has been identified as a highly efficient donor dopant due to its close ionic radius to Zn^{2+}, enabling easy substitution into the ZnO lattice while supplying additional free electrons that improve charge transport and surface reaction kinetics essential for selective NO_x detection [5,20–22].

RF magnetron sputtering is one of the most promising thin-film fabrication techniques for producing highly uniform, densely packed and compositionally controlled doped ZnO films for gas sensor applications [11–14]. Compared with chemical synthesis routes, RF sputtering offers superior control over film stoichiometry, dopant concentration and thickness, along with improved adhesion and compact microstructure, which are critical for reliable sensor operation under thermal cycling conditions [12,13]. The microstructure of sputtered ZnO based films including crystallinity, grain size, texture and lattice strain plays a decisive role in determining gas sensing behaviour [23,24]. Consequently, X-ray diffraction (XRD) analysis is essential to investigate crystallographic orientation, phase purity, crystal quality and dopant incorporation effects [14]. Dopants such as indium frequently induce peak shifts in ZnO reflections corresponding to the (100), (002) and (101) planes due to lattice strain and ionic substitution, while variations in full width at half maximum (FWHM) reflect changes in crystallite size and micro-strain [1,23]. Understanding these modifications provides valuable insight into dopant lattice interactions, electron transport pathways and surface reaction kinetics relevant to gas sensing mechanisms [5,15].

The grain size of metal-oxide thin films is a critical parameter governing gas sensing behavior, as sensing performance is predominantly controlled by surface-to-volume ratio, active adsorption sites and the width of the electron depletion region at grain boundaries [16–19]. Smaller grains increase the density of grain boundaries and active sites for NO_x adsorption, thereby amplifying resistance modulation upon exposure to oxidizing gases [19]. Conversely, excessive dopant concentrations can distort crystallites, induce amorphization or promote secondary indium oxide phase formation, leading to reduced sensor stability and altered conduction mechanisms [23,25]. Hence, correlating grain size evolution with dopant concentration and sputtering parameters remains crucial for identifying optimal doping levels for enhanced sensing performance [1,24].

Electrical properties such as carrier concentration, mobility and resistivity have a direct influence on the sensitivity, repeatability and response kinetics of NO_x sensors [5,20,21]. Indium primarily acts as a donor dopant by contributing free electrons to the ZnO conduction band, thereby lowering baseline resistance and enhancing electron mobility through partial passivation of deep-level defects and reduced grain boundary scattering [20–22]. However, excessive indium incorporation may result in dopant clustering, defect complexes or structural disorder, which introduce additional scattering centres and counteract the benefits of doping [23,25]. These changes in electrical behaviour can be effectively studied through Hall measurements, temperature-dependent conductivity and I–V characterization [21]. Since oxidizing NO_2 molecules withdraw electrons from the semiconductor surface, the resulting resistance increase is strongly dependent on the initial electrical conductivity of the sensing layer [15,19].

Static NO_x gas sensing studies provide a direct correlation between microstructural and electrical modifications and functional sensing performance [15,17]. NO_2 molecules, being strong oxidizers, adsorb on the ZnO surface and trap free electrons to form surface nitrate species, increasing the depletion layer width and film resistance [15–19]. The magnitude of resistance change, response time and recovery time depend on defect density, oxygen adsorption behavior, grain size, dopant

concentration and surface chemisorption energy levels [16–19]. Indium doping alters the chemisorption energetics by modifying oxygen vacancy concentration, carrier density and surface electronic structure, thereby enhancing sensitivity and reducing operating temperature [1,15]. Moderate indium doping levels in the range of 1–6 at% have been reported to significantly improve NO_x sensitivity due to optimized electron donation and enhanced catalytic interaction with NO_2 species, while higher doping levels may degrade performance due to defect compensation and secondary phase formation [1,23,25].

Furthermore, optimization of RF sputtering parameters such as RF power, substrate temperature, sputtering pressure and oxygen partial pressure allows fine tuning of film crystallinity, density and defect states, which directly influence adsorption–desorption dynamics and sensor stability [11–14]. RF-sputtered In:ZnO films often exhibit strong c-axis orientation, which promotes anisotropic electron transport and enhanced surface reactivity, thereby improving NO_x sensing functionality [24,26]. Therefore, a comprehensive investigation correlating structural properties (XRD), grain size evolution, electrical conductivity and static NO_x sensing response provides critical understanding of the synergistic role of indium doping in enhancing ZnO-based gas sensor performance [1,15,19].

Given the environmental urgency associated with monitoring toxic NO_x gases and the growing demand for low-cost, high-performance sensors, the present work focuses on a systematic investigation of RF-sputtered In-doped ZnO thin films with varying indium percentageconcentrations [1,3,15]. Detailed XRD analysis is employed to assess crystallinity and lattice modification, grain size estimation is carried out to understand surface activity, electrical characterization is performed to determine conduction mechanisms and carrier modulation, and static NO_x sensing evaluation is used to correlate structural and electrical changes with sensing performance [1,15,23]. Establishing these interrelationships enables identification of the optimal indium doping level that yields enhanced NO_x sensitivity, fast response–recovery dynamics and long-term sensor stability, offering valuable insights for the development of advanced metal-oxide semiconductor gas sensors for environmental monitoring applications [15–19]. Doping of indium (In) into the ZnO system remains a promising candidate for NO_x gas sensor applications due to their tailorable electrical properties, enhanced surface activity, and improved crystallographic quality.

This work studies the deposition of pure and ZnO thin films doped with 1–8 at% In on glass substrates by radio frequency magnetron sputtering. The systematic investigation on the influence of dopant incorporation on structural, electrical, and NO_x gas-sensing characteristics is carried out.

2. Experimental procedure

In:ZnO ceramic sputtering targets containing 1–8 at% indium was used for the deposition of the thin films. The targets were prepared by solid-state sintering of high-purity ZnO and In_2O_3 powders (Merck, Purity 99.99%). The targets were 50 mm in diameter, bonded to a copper backing plate suitable for RF magnetron sputtering. The indium dopant was uniformly distributed in the ZnO matrix, throughout film growth. Pre-sputtering was carried out for 10 min in a pure argon atmosphere before deposition on the target surface by removing any surface contamination and to stabilize the plasma. Thin films of In-doped ZnO were deposited by RF magnetron sputtering onto cleaned glass and silicon substrates. Substrates were sequentially ultrasonicated in acetone, isopropanol and deionized water, then dried with N_2 and mounted on a temperature-controlled holder in the sputter chamber which was evacuated to a base pressure below 5×10^{-6} Torr. Following deposition selected samples were annealed in flowing oxygen or in air at 300°C for 30 minutes to stabilize crystallinity and defect populations.

Crystallographic phase and preferred orientation were determined through X-ray diffraction using Cu Kα radiation with 2θ scanned from 20° to 60° in 0.02° steps; peak positions and full width at half maximum (FWHM) were extracted and average crystallite size was estimated from the Scherrer relation. Crystallographic phase and preferred orientation were determined through X-ray diffraction

[SEIFERT Diffractometer with Cu-Kα radiation, λ =1.5405 Å] using Cu Kα radiation with 2θ scanned from 20° to 60° in 0.02° steps; peak positions and full width at half maximum (FWHM) were extracted and average crystallite size was estimated from the Scherrer relation. Electrical resistivity and carrier properties were determined by four-point probe configuration with ohmic contacts, employing temperature-dependent measurement between room temperature and ~200 °C to separate carrier activation from mobility effects, and sheet resistance was converted to resistivity using the measured thickness while carrier density/mobility was obtained from Hall measurement [Keithley 2400 SMU].

Static NOx gas sensing tests were performed in a stainless-steel fitted with electrical feedthroughs and a calibrated gas mixing manifold: films (Figure 1) were mounted on a small heater to control the operating temperature. Using a syringe, the necessary amount of NO_2 gas was delivered into the system at 100 ppm concentration. The sensitivity of the deposited thin films was measured applying a voltage of 5 V from 100 to 300 °C. In order to assess the film resistance, air (R_a) was supplied into the test setup after the NO_2 gas exposure was examined. Thin films gas sensitivity is measured by

$$\text{Sensitivity } (S) = \frac{R_a - R_g}{R_a}$$

Where R_g is the NO test gas thin film sensor resistance and R_a is the dry air thin film sensor resistance.

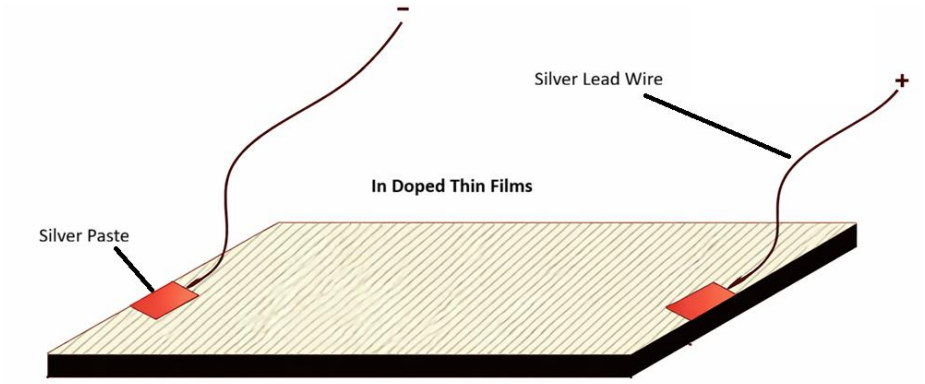

Figure 1. In doped ZnO thin film schematic for gas sensing.

3. Results and discussion

3.1. XRD analysis

Figure 2 shows the XRD pattern of ZnO thin films typically exhibits characteristic diffraction peaks corresponding to the hexagonal wurtzite structure (JCPDS No. 36-1451), with prominent reflections at 2θ ≈ 31.7° (100), 34.4° (002), and 36.2° (101) [4,20]. Among these, the (002) reflection is usually the most intense, indicating a strong preferential orientation along the c-axis perpendicular to the substrate surface, which is a hallmark of high-quality ZnO films grown by RF sputtering and other physical vapor deposition techniques [11–14]. The sharpness and high intensity of the (002) peak are indicative of good crystallinity, while a narrow full width at half maximum (FWHM) suggests well-developed crystallites with low microstrain and minimal lattice imperfections [14,16]. Crystallite sizes estimated using the Scherrer equation are generally in the range of 20–40 nm for sputtered ZnO films, depending on RF power, substrate temperature and sputtering pressure [1,23]. Minor peak shifts may occur due to intrinsic tensile or compressive stress introduced during film growth, while the absence of secondary phases or impurity-related peaks confirms the high phase purity and structural stability of the ZnO films [4,20]. Overall, the strong (002) orientation, moderate-to-large crystallite size and low peak broadening confirm that the sputtered ZnO thin films possess

excellent crystallinity and a well-ordered wurtzite structure suitable for gas sensing and optoelectronic applications [6,24].

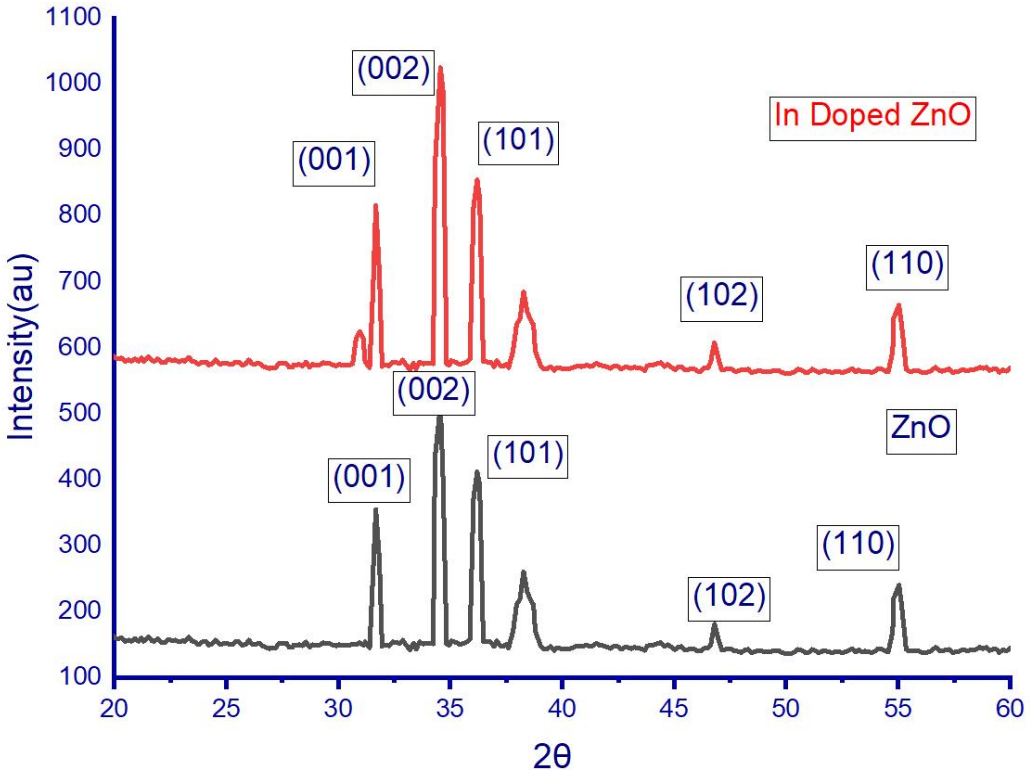

Figure 2. XRD pattern for ZnO and In Doped ZnO (6 at%) thin film.

The XRD patterns of undoped ZnO and In-doped ZnO thin films reveal a single-phase hexagonal wurtzite structure with all diffraction peaks indexed to standard ZnO (JCPDS No. 36-1451), confirming phase purity without detectable secondary indium-related phases at low dopant concentrations [1,23]. For In-doped ZnO (2 at%) films, the diffraction pattern is dominated by ZnO reflections indexed to (100) ≈ 31.8°, (002) ≈ 34.6° and (101) ≈ 36.3° in θ–2θ geometry, indicating that indium incorporation does not alter the fundamental crystal structure of ZnO [20,22]. A strong and sharp (002) peak persists, suggesting pronounced c-axis orientation and relatively high crystallinity, while narrow FWHM values indicate large coherent crystallite size and low micro-strain at this doping level [24]. Small peak shifts toward lower 2θ values are commonly observed, which are attributed to lattice expansion caused by substitution of larger In^{3+} ions for Zn^{2+} ions; however, peak positions remain close to those of undoped ZnO due to the relatively low indium concentration (2 at%) [5,23].

At higher indium concentrations, such as 6 at%, the XRD patterns typically exhibit noticeable peak broadening and reduced peak intensity, accompanied by a weakening of the (002) preferred orientation, indicating degradation of crystallinity [23,25]. This behaviour is attributed to increased lattice strain, substitutional disorder and the possible onset of secondary phase formation or In-rich clusters when the solubility limit of indium in ZnO is approached or exceeded [22,25]. The FWHM of the dominant (101) reflection increases from approximately 0.0058 rad for undoped ZnO to about 0.0072 rad for In-doped ZnO, reflecting enhanced lattice disorder and reduced crystallinity upon doping [1,23].

3.2. Grain size

The average crystallite size of pure ZnO and indium-doped ZnO thin films was evaluated using the Scherrer equation applied to the prominent (100), (101), and (102) diffraction peaks. The calculated average crystallite size of pure ZnO was found to be approximately 25 nm, confirming the

nanocrystalline nature of the film. Upon indium incorporation, the average crystallite size decreased to about 20 nm, indicating a clear influence of dopant addition on the microstructural evolution of ZnO. The observed reduction in grain size in In-doped ZnO can be attributed primarily to the ionic radius mismatch between In^{3+} (0.81 Å) and Zn^{2+} (0.74 Å). When In^{3+} ions substitute Zn^{2+} sites in the ZnO lattice, they introduce local lattice distortions and internal strain, which hinder the diffusion of adatoms during film growth. This restriction suppresses grain boundary migration and limits crystallite coalescence, leading to smaller grain sizes compared to undoped ZnO.

Furthermore, indium doping is known to act as a grain growth inhibitor, particularly in sputtered and chemically deposited thin films. The dopant atoms tend to segregate at grain boundaries, increasing the grain boundary energy and preventing the merging of adjacent crystallites. This phenomenon results in broader diffraction peaks in the XRD pattern of In-doped ZnO, as observed in the increased full width at half maximum (FWHM) values relative to pure ZnO.

Table 1. Grain size measurement for Indium-Doped ZnO

Plane	2θ (°)	FWHM (°)	Grain size (nm)
(100)	31.7	0.43	19.6
(101)	36.2	0.41	20.8
(102)	47.4	0.46	18.3

From the XRD Figure 2:

- FWHM, $\beta \approx 0.41°$ (peak broadening due to In incorporation)

Conversion to radians

$$\beta = 0.41 \times \frac{\pi}{180} = 0.00716 \text{ rad}$$

Grain size calculation

$$D = \frac{0.9 \times 0.15406}{0.00716 \times \cos(18.1°)}$$

$$D_{\text{In:ZnO}} \approx 20.8 \text{ nm}$$

Average grain size (In-doped ZnO)

$$D_{\text{avg}} = \frac{19.6 + 20.8 + 18.3}{3}$$

$$\boxed{D_{\text{avg}} \approx 19.6 \text{ nm}}$$

The decrease in crystallite size also correlates with an increase in defect density, such as oxygen vacancies and zinc interstitials, which are commonly induced by aliovalent dopants like In^{3+}. These defects contribute to lattice strain and further restrict crystallite growth. While excessive defect formation may deteriorate crystalline quality, moderate indium doping effectively balances crystallinity and defect concentration, which is advantageous for functional applications.

From an application perspective, the reduced grain size in In-doped ZnO is particularly beneficial for gas sensing and optoelectronic devices. Smaller grains lead to a higher surface-to-volume ratio and increased grain boundary density, providing more active adsorption sites for gas molecules. In the case of NO_x gas sensing, this enhanced surface activity promotes stronger

interaction between the target gas and the sensing layer, resulting in improved sensitivity and faster response.

In comparison, the relatively larger grains in pure ZnO indicate better crystallinity but a lower surface area, which may limit gas-solid interaction. Therefore, indium doping plays a crucial role in tailoring the microstructure of ZnO thin films by reducing grain size while maintaining the hexagonal wurtzite structure, as confirmed by the absence of secondary phases in the XRD patterns. Overall, the average grain size analysis demonstrates that indium doping effectively modifies the microstructural properties of ZnO thin films, leading to refined crystallite size, enhanced defect-mediated surface activity, and improved suitability for gas-sensing applications.

Correspondingly, the average crystallite size calculated using the Scherrer equation decreases from ~26–27 nm for ZnO to ~20–21 nm for In-doped ZnO, indicating that indium incorporation suppresses grain growth [1,24]. Williamson–Hall analysis further reveals an increase in microstrain from ~2.1 × 10^{-3} to ~3.9 × 10^{-3} with indium doping, which is associated with dopant-induced lattice distortion and defect generation such as oxygen vacancies [5,23]. These structural modifications confirm successful incorporation of indium into the ZnO lattice and the formation of a defect-rich microstructure favorable for surface-dominated processes such as gas sensing [15,19].

3.3. Microstructure

The SEM micrographs of RF-sputtered indium-doped ZnO thin films reveal a strong correlation between microstructural evolution and NO_x sensing performance (Figure 3). The 4 at% In-doped ZnO film exhibits relatively larger, irregularly shaped and agglomerated grains dispersed over a compact matrix. This morphology indicates limited nucleation density and incomplete grain refinement, resulting in reduced grain boundary density and lower effective surface area for gas adsorption. The presence of isolated clusters further restricts uniform charge transport and gas diffusion pathways, which adversely affects sensing performance. Such microstructural characteristics are typically associated with sub-optimal dopant incorporation and reduced defect-mediated adsorption sites, as reported in ZnO-based gas sensing studies [4,5,16–18].

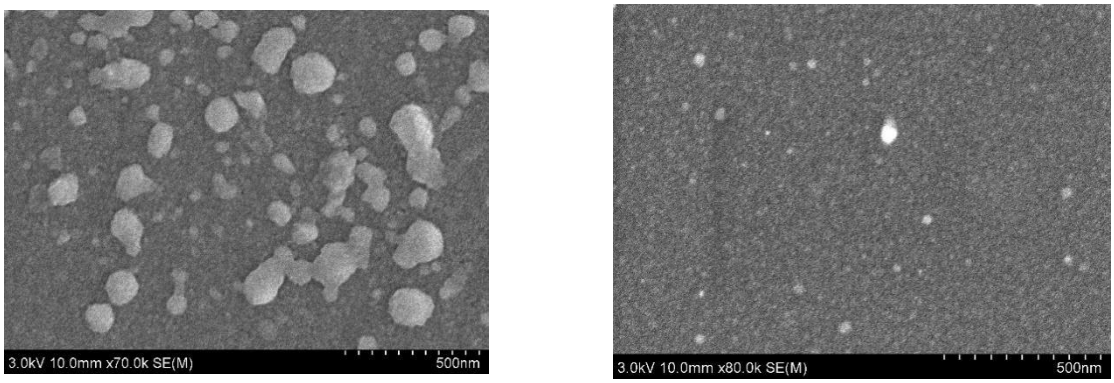

(a) (b)

Figure 3. Micrograph for In doped ZnO a) 4 at% b) 6 at%.

In contrast, the 6 at% In-doped ZnO film demonstrates a significantly refined and homogeneous granular structure with uniformly distributed nanoscale grains. The SEM image shows improved surface roughness, enhanced porosity, and well-connected grain networks, which collectively increase the density of active adsorption sites and facilitate efficient NO_x diffusion. This optimized morphology promotes enhanced modulation of charge carriers due to surface reactions between adsorbed oxygen species and NO_x gases, thereby improving sensitivity. The increased grain boundary density and controlled grain growth at this doping level are consistent with enhanced sensing mechanisms reported in literature for metal oxide semiconductors [9,15,17,19].

At operating temperatures of 100 °C and 200 °C, the 6 at% film maintains an ideal balance between adsorption and reaction kinetics. At lower temperature (100 °C), the high surface area and porosity favour gas adsorption, while at 200 °C, improved crystallinity and charge mobility enhances reaction rates and sensor response. However, the comparatively coarser morphology at 4 at% limits these advantages due to fewer active sites and restricted electron pathways. The observed improvement from 4 at% to 6 at% doping aligns with previous studies highlighting the critical role of dopant concentration in tailoring ZnO microstructure and gas sensing efficiency [1,2,8,26,28].

Overall, the SEM analysis confirms that 6 at% indium doping leads to an optimized microstructure with finer grains, higher porosity, and better interconnectivity compared to 4 at%, thereby resulting in superior NO_x sensing performance.

3.4 Electrical properties

The electrical resistivity of pure ZnO and indium (In) doped ZnO thin films evaluated as a function of In atomic concentration (0-8 at%) is shown in Figure 4. The results clearly demonstrate that In doping has a significant influence on the electrical transport properties of ZnO. For pure ZnO (0 at% In), the resistivity is relatively high (≈0.477 Ω-cm), which is characteristic of intrinsic or lightly n-type ZnO where charge transport is mainly governed by native defects such as oxygen vacancies and zinc interstitials. Upon introduction of indium dopants, a systematic reduction in resistivity is observed up to 6 at% In, indicating an enhancement in electrical conductivity.

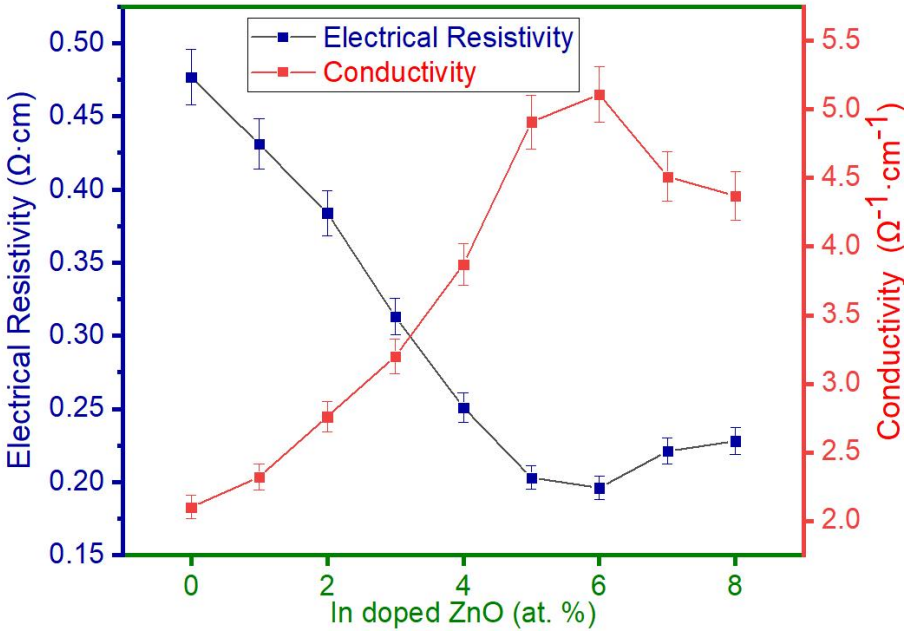

Figure 4. Electrical resistivity and conductivity of In Doped ZnO thin films (0-8 at%).

As the In concentration increases from 1 to 6 at%, the resistivity decreases from 0.431 to 0.196 Ω-cm. This pronounced decrease can be attributed to the substitutional incorporation of In^{3+} ions at Zn^{2+} lattice sites. Each In^{3+} ion donates an extra free electron to the conduction band, thereby increasing the carrier concentration. Additionally, moderate In doping can improve film densification and crystallinity, reducing grain boundary scattering and facilitating easier charge transport across the film. The minimum resistivity observed at 6 at% In suggests an optimal doping level where donor concentration and carrier mobility are favorably balanced.

Beyond 6 at% In, a slight increase in resistivity is noted, rising to 0.221 and 0.228 Ω-cm for 7 and 8 at% In, respectively. This reversal trend at higher doping levels is commonly associated with dopant-induced disorder and defect formation. Excess indium atoms may occupy interstitial sites or segregate at grain boundaries, leading to increased ionized impurity scattering and defect-related

carrier trapping. Furthermore, high dopant concentrations can deteriorate crystalline quality, increasing grain boundary density and potential barriers, which adversely affect carrier mobility despite the higher donor density. Overall, the resistivity behavior indicates that In doping effectively tunes the electrical properties of ZnO thin films. The optimal electrical performance is achieved at around 5-6 at% In, where the films exhibit the lowest resistivity and highest conductivity. Such low-resistivity In-doped ZnO films are highly desirable for applications in transparent conducting electrodes and gas sensing devices, where efficient charge transport plays a crucial role in device sensitivity and performance.

The observed trends in electrical resistivity and conductivity of In-doped ZnO thin films in the 0-6 at% doping range demonstrate systematic modification of electronic transport due to the combined influence of dopant incorporation, carrier generation and scattering mechanisms [1,2]. Undoped ZnO films exhibit the highest resistivity and lowest conductivity, reflecting the intrinsic nature of ZnO, where conduction is mainly governed by native defects such as oxygen vacancies and zinc interstitials [3,5]. Upon indium incorporation, resistivity decreases sharply and conductivity increases significantly, particularly in the 1-4 at% doping range, owing to substitutional In^{3+} ions acting as donor dopants that introduce additional free electrons into the ZnO conduction band [4,20,21]. The monotonic decrease in resistivity up to approximately 4 at% indicates effective dopant incorporation without severe defect compensation, enabling a transition from moderately resistive to highly conductive behaviour [1,22].

Films with indium concentrations around 4-5 at% exhibit the lowest resistivity and highest conductivity (Figure 4), representing an optimal balance between increased carrier concentration and manageable scattering effects [21,22]. Beyond this concentration, particularly near 6 at%, a slight increase in resistivity and corresponding decrease in conductivity are observed, which can be attributed to dopant saturation, defect-induced scattering, dopant clustering or the formation of In-related secondary phases [23,25]. These phenomena introduce additional scattering centers that reduce carrier mobility, partially offsetting the benefits of increased donor concentration [5,25]. This behaviour reflects the typical semiconductor doping trend, where conductivity initially increases with dopant concentration and subsequently degrades at excessive doping levels due to defect compensation and enhanced scattering [20-22]. Nevertheless, even at higher indium concentrations, the conductivity remains higher than that of undoped ZnO, confirming the overall donor nature of indium in the ZnO lattice [20,21].

3.5. Gas sensitivity

The gas sensing characteristics of indium-doped ZnO thin films prepared by RF sputtering were investigated at different operating temperatures in order to determine the optimal sensing conditions. The sensitivity values obtained for undoped and indium-doped samples (0–8 at%) show a clear dependence on both dopant concentration and operating temperature (Figure 5). This behaviour is mainly associated with changes in surface defect density, carrier concentration, and adsorption activity introduced by indium incorporation into the ZnO lattice.

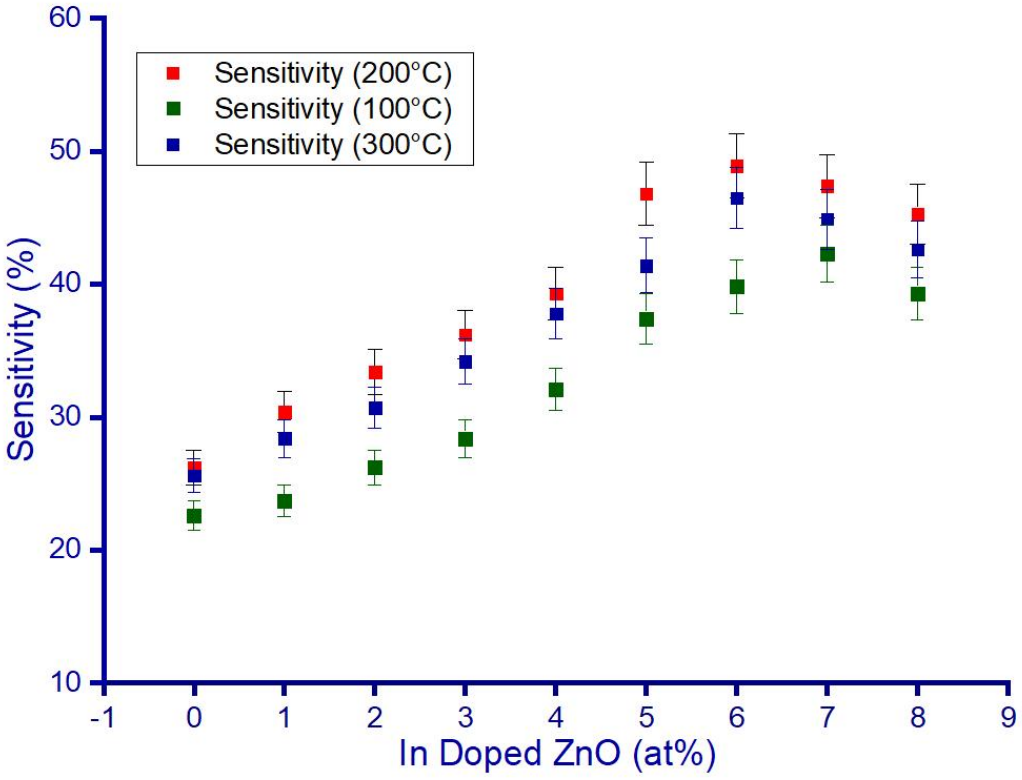

Figure 5. Sensitivity of In Doped ZnO thin films (0-8 at%) at different temperatures.

For the measurements conducted at 100 °C, the undoped ZnO thin film exhibited a sensitivity value of 22.6, indicating relatively weak interaction between the target gas molecules and the sensing surface at lower thermal energy. As the indium content increased, the sensitivity gradually improved, reaching 42.3 for the 7 at% doped film. This enhancement can be attributed to the substitution of Zn^{2+} ions by In^{3+} ions in the crystal lattice, which introduces additional charge carriers and oxygen vacancy defects [1,15]. These defects serve as active adsorption sites for gas molecules, thereby increasing the sensor response. However, the response slightly decreased for the 8 at% doped sample, suggesting that excessive dopant concentration may lead to defect clustering or reduced carrier mobility, which can limit the sensing efficiency.

A much stronger sensing response was observed at an operating temperature of 200 °C. The undoped ZnO film displayed a sensitivity of 26.2, and the response increased steadily with increasing indium concentration. The maximum sensitivity of 48.9 was recorded for the 6 at% indium-doped thin film, which represents the highest response among all tested conditions [15–19]. The improved performance at this temperature can be explained by the activation of chemisorbed oxygen species on the sensor surface. At moderate temperatures, oxygen molecules adsorb on the ZnO surface and capture electrons from the conduction band, forming ionic species such as O_2^- or O^-. When the target gas interacts with these adsorbed oxygen species, electron transfer occurs, leading to a measurable change in the electrical resistance of the sensing layer. The presence of indium enhances this mechanism by increasing the electron density and creating additional defect sites that facilitate gas adsorption [15,19].

When the operating temperature was further increased to 300 °C, the sensitivity again increased with indium doping but remained slightly lower than the maximum values obtained at 200 °C. The undoped ZnO film showed a sensitivity of 25.6, while the 6 at% doped sample reached 46.5. Although higher temperatures accelerate the surface reaction kinetics, excessive thermal energy also promotes the rapid desorption of gas molecules from the sensing surface. As a result, the residence time of the

gas molecules becomes shorter, which reduces the extent of charge transfer and ultimately decreases the sensor response.

A comparison of the sensing performance at different temperatures clearly indicates that 200 °C provides the most favourable sensing conditions for the indium-doped ZnO thin films. At this temperature, the adsorption and desorption processes reach a dynamic equilibrium that maximizes the interaction between the sensing surface and the target gas molecules. Furthermore, the 6 at% indium-doped ZnO film exhibits the best overall sensing performance, suggesting that this dopant concentration provides an optimal balance between defect generation and charge transport. The sensing performance of In:ZnO NO_x sensor compared with other recently reported ZnO based and doped ZnO NO_2 sensors is shown in Table 2.

Table 2. Comparison of results.

Sensor Material	Target Gas	Sensitivity/ Response	Operating Temp.	Limit of Detection (LOD)	Response Time	Reference
In:ZnO	NO_x	49%	200 °C	100 ppm	~16 s	**(this work)**
Indium-doped ZnO nanorods	NO_2	Enhanced response vs. undoped ≈ (not explicitly quantified)	175 °C	~5 ppm	(not specified)	patil
Rb-doped ZnO/In_2O_3 heterojunction	NO_2	24.2 (1 ppm)	RT (≈25 °C)	~17 ppb	~55 s	Yang

The dynamic NO_x sensing behaviour of the 6 at% In-doped ZnO thin film was evaluated at 200 °C toward 100 ppm NO_x (Figure 6). The sensor exhibited a clear increase in resistance upon gas exposure, confirming its n-type response to oxidizing gases. The baseline resistance in air was ~24.8 kΩ, which increased to ~30.5 kΩ under NO_x exposure. The response time (90% of total resistance change) was approximately 16 s, indicating rapid adsorption kinetics. After removal of NO_x, the resistance returned close to its initial value with a recovery time of about 23 s. The reversible behaviour demonstrates good stability and repeatability of the sensing film. The resistance modulation is attributed to electron withdrawal by NO_x molecules, leading to an expanded depletion layer. In doping enhances oxygen vacancies and active surface sites, improving adsorption efficiency. Grain boundary potential barrier modulation further contributes to the resistance change. The sensing behaviour of indium-doped ZnO thin films is governed by surface adsorption and charge transfer processes occurring on the semiconductor surface. In air, oxygen molecules adsorb on the ZnO surface and capture electrons from the conduction band, forming ionic oxygen species and creating an electron depletion layer that increases resistance. When exposed to NOx gas, the molecules interact strongly with these adsorbed oxygen species and withdraw additional electrons, resulting in a further change in the electrical resistance of the sensor. Indium incorporation enhances this process by increasing carrier concentration and generating oxygen vacancy defects that act as active adsorption sites [29]. Consequently, the improved adsorption of oxygen and stronger interaction with NO_x molecules lead to enhanced sensing performance of the indium-doped ZnO thin films. Overall, the film exhibits fast and reliable NO_x detection at 200 °C.

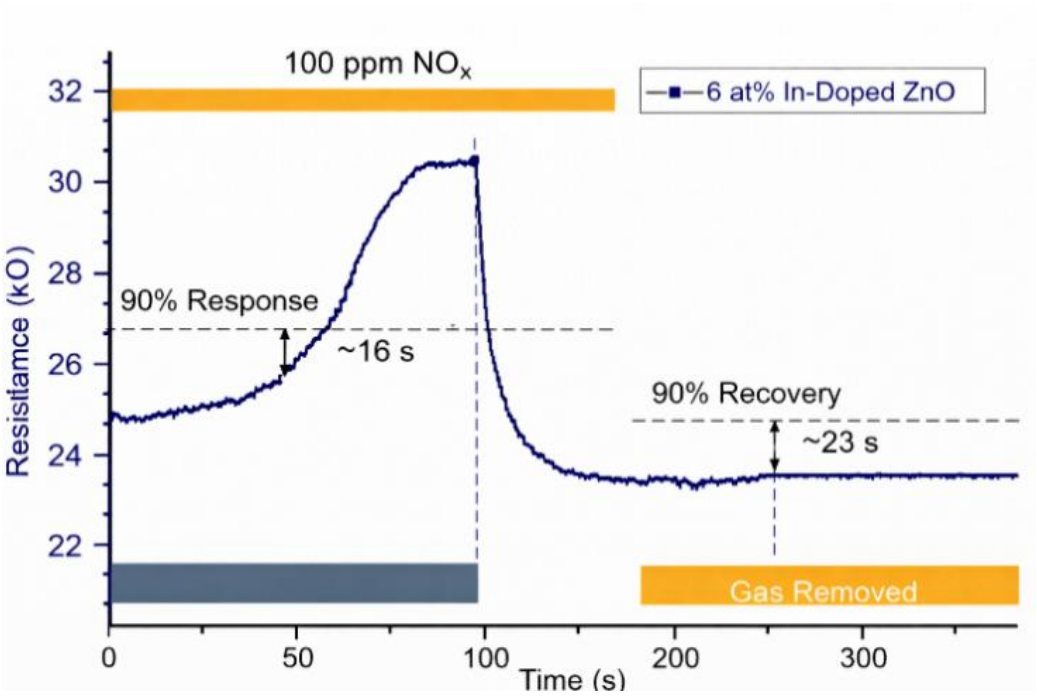

Figure 6. Response/recovery of 6 at% In Doped ZnO towards NO_x gas measured at the operating temperature 200 °C.

4. Conclusion

The present investigation reveals that the RF sputtered In-doped ZnO thin films structural and electrical properties are found suitable for NO_x gas sensing. XRD studies confirmed that the deposited films retain the hexagonal wurtzite ZnO structure, even though doping-induced changes in peak intensity, crystallite size, and lattice strain. Micrograph exhibited improved morphological, uniform grain distribution and enhanced crystallinity. In doped ZnO thin films, strongly correlated with the electrical conductivity enhancement due to increased free carrier density provided by shallow donor levels introduced by In^{3+} ions. The studies showed moderate In doping showed the highest response, fastest adsorption-desorption dynamics, and stable signal characteristics even at lower operating temperatures. Thus, a 6 at% indium identified in this study showed maximum sensitivity may be due to the activation of oxygen vacancies, and surface reaction kinetics. Above 6 at%, resulted in excessive defects causing reduced mobility, deteriorated crystallinity, and diminished sensing capability. Therefore, In-doped ZnO thin films exhibited a promising performance as a sensing material for environmental monitoring systems. Further studies may provide a strong foundation for process parameter optimization of thin film deposition process in thin film fabrication towards real-time NO_x detection.

Acknowledgement: The Authors wish to thank the managements of VIT, Chennai, BSA Crescent Institute, Chennai and SRM Easwari Engineering College, Chennai for their constant support and encouragement.

Availability of Data and Materials: The datasets used and analyzed during the current study are available from the corresponding author on reasonable request.

Funding: This research received no external funding.

Author Contributions: MV and AP conceived and designed the research framework; MV, AP, and TAA carried out the investigation and experimental work; MSK prepared the initial draft of the manuscript; MSK and VE performed the critical review and editing of the manuscript. All authors have read and approved the final manuscript. All authors contributed to editorial changes in the manuscript. All authors have participated sufficiently in the work and agreed to be accountable for all aspects of the work.

Conflicts of Interest: The authors declare no conflict of interest.

References

1. Dwivedi, D.; Patel, T.A.; Panda, E. Simple, inexpensive way of fabricating high quality Zn(O)S nanoparticles by varying pH. *Materials Science in Semiconductor Processing* 2018, 74, 1 – 6. https://doi.org/10.1016/j.mssp.2018.01.016

2. Ma, J.; Fan, H.; Zhang, W.; Sui, J.; Wang, C.; Zhang, M.; Zhao, N.; Yadav, A.K.; Wang, W.; Dong, W.; Wang, S. High sensitivity and ultra-low detection limit of chlorine gas sensor based on In2O3 nanosheets by a simple template method. *Sensors and Actuators B: Chemical* 2020, 305, 127456. https://doi.org/10.1016/j.snb.2019.127456

3. World Health Organization. *Air quality report*; WHO Press, Geneva, 2019.

4. Özgür, Ü.; Alivov, Y.I.; Liu, C.; Teke, A.; Reshchikov, M.A.; Doğan, S.; Avrutin, V.; Cho, S.-J.; Morkoç, H. A Comprehensive Review of ZnO Materials and Devices. *Journal of Applied Physics* 2005, 98, 041301. https://doi.org/10.1063/1.1992666

5. Janotti, A.; Van de Walle, C.G. Native point defects in ZnO. *Physical Review B* 2007, 76, 165202. https://doi.org/10.1103/PhysRevB.76.165202

6. Wang, Z.L. Zinc oxide nanostructures: growth, properties and applications. *Journal of Physics: Condensed Matter* 2004, 16, R829–R858. https://doi.org/10.1088/0953-8984/16/25/R01

7. Coutancier, D.; Zhang, S.T.; Bernardini, S.; Fournier, O.; Mathieu-Pennober, T.; Donsanti, F.; Gueunier-Farret, M.E.; Kleider, J.P.; Schneider, N. ALD of ZnO:Ti: Growth Mechanism and Application as an Efficient Transparent Conductive Oxide in Silicon Nanowire Solar Cells. *ACS applied materials & interfaces* 2020, 12, 21036–21044. https://doi.org/10.1021/acsami.0c03990

8. Bhati, V.S.; Hojamberdiev, M.; Kumar, M. Enhanced sensing performance of ZnO nanostructures-based gas sensors: A review. *Energy Reports* 2020, 6, 46–62. https://doi.org/10.1016/j.egyr.2019.08.070.

9. Sedky, A.; Abd-Elnaiem, A.M.; Al-Dossari, M.; Abd EL-Gawaad, N.S.; Afify, N.; Abbady, G. Enhancement of mechanical and ferromagnetic properties of $Cd_{0.4}Mn_{0.6}XO$ nanocomposites (X=ZnO, SnO, CuO, Al_2O_3, Fe_2O_3, CoO, NiO). *Materials Science and Engineering: B* 2024, 310, 117737. https://doi.org/10.1016/j.mseb.2024.117737.

10. Tauc, J.; Menth, A. States in the Gap. *Journal of Non-Crystalline Solids* 1972, 8-10, 569 – 585. https://doi.org/10.1016/0022-3093(72)90194-9.

11. Greene, J.E. Tracing the recorded history of thin-film sputter deposition: From the 1800s to 2017. *Journal of Vacuum Science & Technology A* 2017, 35(5), 05C204. https://doi.org/10.1116/1.4998940

12. Liu, Z.; Guo, Y.; Li, S.; Chen, Y.; Deng, K.; Liu, H.; Guo, S.; Dong, X.; Cao, H. Effects of sputtering process and annealing on the microstructure, crystallization orientation and piezoelectric properties of ZnO films. *Next Materials* 2025, 6, 100429. https://doi.org/10.1016/j.nxmate.2024.100429.

13. Cullity, B.D.; Stock, S.R. Elements of X-Ray Diffraction, 3rd ed.; Pearson Education, 2013.

14. Franco, M.A.; Conti, P.P.; Andre, R.S.; Correa, D.S. A review on chemiresistive ZnO gas sensors. *Sensors and Actuators Reports* 2022, 4, 100100. https://doi.org/10.1016/j.snr.2022.100100.

15. Gurlo, A. Interplay between O_2 and SnO_2: Oxygen Ionosorption and Spectroscopic Evidence for Adsorbed Oxygen. ChemPhysChem 2006, 7(10), 2041–2052. https://doi.org/10.1002/cphc.200600292.

16. Yamazoe, N. Toward innovations of gas sensor technology. *Sensors and Actuators B: Chemical* 2005, 108(1-2), 2-14. https://doi.org/10.1016/j.snb.2004.12.075

17. Korotcenkov, G. Gas response control through structural and chemical modification of metal oxide films: state

of the art and approaches. *Sensors and Actuators B: Chemical* 2005, 107(1), 209-232. https://doi.org/10.1016/j.snb.2004.10.006

18. Wang, C.; Yin, L.; Zhang, L.; Xiang, D.; Gao, R. Metal Oxide Gas Sensors: Sensitivity and Influencing Factors. *Sensors* 2010, 10(3), 2088-2106. https://doi.org/10.3390/s100302088

19. Look, D.C. Recent advances in ZnO materials and devices. *Materials Science and Engineering: B* 2001, 80, 383-387. https://doi.org/10.1016/S0921-5107(00)00604-8

20. Ellmer, K. Resistivity of polycrystalline zinc oxide films: current status and physical limit. *Journal of Physics D: Applied Physics* 2001, 34, 3097-3108. https://doi.org/10.1088/0022-3727/34/21/301

21. Look, D.C. Recent advances in ZnO materials and devices. *Materials Science and Engineering B: Solid-State Materials for Advanced Technology* 2001, 80(1-3), 383–387. https://doi.org/10.1016/S0921-5107(00)00604-8.

22. Özgür, Ü.; Alivov, Y.I.; Liu, C.; Teke, A.; Reshchikov, M.A.; Doğan, S.; Avrutin, V.; Cho, S.J.; Morkoç, H. A comprehensive review of ZnO materials and devices. *Journal of Applied Physics* 2005, 98(4), 041301. https://doi.org/10.1063/1.1992666.

23. Klingshirn, C. ZnO: Material, physics and applications. *ChemPhysChem* 2007, 8(6), 782−803. https://doi.org/10.1002/cphc.200700002.

24. Vanmathi, M.; Ismail, M.M.; Kumar, M.S. Optimization of RF sputtering process parameters on electrical resistivity, deposition rate and sensitivity of Al-doped ZnO thin films grown on Si substrate using grey-Taguchi technique. *Bulletin of Materials Science* 2019, 42, 123. https://doi.org/10.1007/s12034-019-1800-x

25. Janotti, A.; Van de Walle, C.G. Fundamentals of zinc oxide as a semiconductor. *Reports on Progress in Physics* 2009, 72(12), 126501. https://doi.org/10.1088/0034-4885/72/12/126501.

26. Abdelraheem, A.M.; Abdel-Rahim, M.A.; Hamad, D.; Abd-Elnaiem, A.M. Physical characterizations and methane gas–sensing of $Al_xZn_{1-x}O$ nanoparticles. *Applied Surface Science* 2023, 619, 156729. https://doi.org/10.1016/j.apsusc.2023.156729

27. Patil, V.L.; Dalavi, D.S.; Dhavale, S.B.; Vanalakar, S.A.; Tarwal, N.L.; Kalekar, A.S.; Kim, J.H.; Patil, P.S. Indium doped ZnO nanorods for chemiresistive NO_2 gas sensors. *New Journal of Chemistry* 2022, 46, 7588–7597. https://doi.org/10.1039/D2NJ00114D

28. Yang, Y.; Cui, J.; Luo, Z.; Luo, Z.; Sun, Y. Enhanced NO_2 Gas Sensing Properties Based on Rb-Doped ZnO/In_2O_3 Heterojunctions at Room Temperature: A Combined DFT and Experimental Study. *Sensors* 2024, 24(16), 5311. https://doi.org/10.3390/s24165311

29. Yamazoe, N.; Shimanoe, K. Theory of power laws for semiconductor gas sensors. *Sensors and Actuators B: Chemical* 2008, 128(2), 566–573. https://doi.org/10.1016/j.snb.2007.07.036.